Thermal Motion and Energetics of Self-Assembled Domain Structures: Pb on Cu(111)

R. van Gastel,[1] R. Plass,[1] N. C. Bartelt,[2] and G. L. Kellogg[1]
[1]*Sandia National Laboratories, Albuquerque, New Mexico 87185-1415, USA*
[2]*Sandia National Laboratories, Livermore, California 94551-0969, USA*
(Received 30 December 2002; published 30 July 2003)

Low energy electron microscope measurements of the thermal motion of 50–200 nm diameter Pb islands on Cu(111) are used to establish the nature and determine the strength of interactions that give rise to self-assembly in this two-dimensional, two-phase system. The results show that self-assembled patterns arise from a temperature-independent surface stress difference of approximately 1.2 N/m between the two phases. With increasing Pb coverage, the domain patterns evolve in a manner consistent with models based on dipolar repulsions caused by elastic interactions due to a surface stress difference.

DOI: 10.1103/PhysRevLett.91.055503 PACS numbers: 81.16.Dn, 68.35.Md, 68.37.Nq, 68.47.De

Over the past two decades, there have been many observations of two-dimensional, self-assembled, domain patterns reported in the literature [1–16]. Ordered arrays of dots (called bubble or droplet phases), alternating rows of domains (called stripe phases), and interesting variations of these (e.g., two-dimensional labyrithine patterns) are seen in systems as different as ferromagnetic thin films [1–6], Langmuir monolayers at the air-water interface [7–10], and adsorbed atoms on solid surfaces [11–15]. The common feature in these widely varying systems is a competition between short-range attractive and long-range repulsive (electrostatic, magnetostatic, or elastic) interactions that leads to stabilization of domains with characteristic feature dimensions. Although thermodynamic properties of domain structures resulting from competing interactions has been the subject of many theoretical studies [1,2,4,7,9,10,17–24], quantitative information on the forces that drive pattern formation is lacking because it is difficult to measure forces on the length scale of self-assembly directly.

In this Letter, we overcome this difficulty by using thermal fluctuations to quantify the interactions that drive two-dimensional self-assembly of domains of Pb surface alloys on Cu(111). When Pb is deposited on Cu(111) at Pb coverages up to 0.22 ML (here one monolayer is defined as one Pb atom per surface Cu atom), Pb atoms that are deposited are incorporated in the surface and form a disordered surface alloy. At coverages exceeding 0.22 ML, the surface alloy phase coexists with a phase that consists of a monolayer of Pb on top of a clean Cu(111) surface, referred to as the overlayer phase. The atomic structures of these two phases and their thermodynamic properties have been well characterized by a variety of techniques [25–29]. The Pb overlayer phase completely covers the surface at 0.56 monolayer. It has a lattice constant close to 4/3 that of the Cu substrate although the precise ratio varies with temperature.

Recent studies with the low energy electron microscope (LEEM) show that the patterns formed by the two types of domains in this system encompass the complete range of phases expected when long- and short-range forces compete [16,30]. As the Pb concentration increases, the domain structure evolves from patterns of approximately circular overlayer islands (2D droplets) to alternating rows of the two phases (stripes) to circular surface alloy islands with the two phases reversed (inverted 2D droplets) (see Fig. 1). This agrees with the predictions of calculations and simulations for two-phase systems with $1/r^3$ dipolar interactions between domain boundaries [7,9,17–24]. Reference [16] suggested that the self-assembly in this system is due to elastic relaxations caused by a stress difference between the two surface phases of Pb on Cu(111). To establish this hypothesis, one needs to be able to measure the underlying long-ranged interactions. We do this here by using the real-time imaging capabilities of the LEEM to analyze the thermal motion of 2D droplets and inverted 2D droplets. We find that the measured strength of the interactions corresponds to a reasonable value of the difference between the surface stresses of the two phases. This supports the conclusion that the forces behind the self-assembly are caused by elastic relaxations.

To quantify the thermodynamic properties of the Pb/Cu(111) system further, we use LEEM to measure the Pb coverages at which the 2D droplet-to-stripe phase transitions occur and to measure the coverage dependence of the variation in domain boundary density. The results of these measurements are also consistent with models

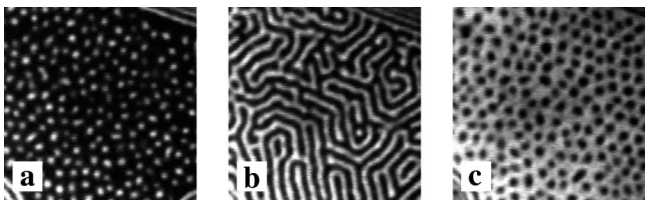

FIG. 1. Surface domain self-assembly evolution during Pb deposition on Cu(111). LEEM bright-field micrographs of the Cu(111) surface with (a) a 2D droplet, (b) a striped, and (c) an inverted 2D-droplet pattern. Images were taken at an electron energy of 18 V where the overlayer phase appears bright and the surface alloy phase appears dark (field of view is 1.8 μm).

and simulations based on competing attractive and repulsive dipolar interactions [12,23], and thus they support the assumption of $1/r^3$ interactions in the analysis of 2D-droplet motion.

Figure 1 illustrates the behavior of the two Pb-Cu surface phases with increasing Pb coverage. The images were obtained using a commercial LEEM of Bauer's design [31]. The details of the experimental setup, the procedures to prepare clean Cu surfaces, and the imaging methods are published elsewhere [32]. As reported earlier [16], the continuous evolution of phases in Fig. 1 follows the trend from 2D droplets to stripes to inverted 2D droplets expected when long-ranged repulsions and short-ranged attractions compete. What is not evident from the static images of Fig. 1 is that the features shown are undergoing considerable thermal motion. We have analyzed this motion through an automated measurement of the center-of-mass (c.m.) of the 2D droplets. For example, in Fig. 2(a), we plot the c.m. trajectories of 2D droplets at 595 K. At higher temperatures and smaller 2D-droplet densities, the thermal motion is even larger. A detailed examination of this dynamic behavior thus permits quantitative tests of existing theories and a determination of the key force parameters involved in the self-assembly process, as we now discuss.

First, we gauge the strength of the interactions by analyzing the thermal motion in a dense 2D-droplet configuration. Because of the significant order in these arrays, each 2D droplet fluctuates around its "equilibrium" position. The size of the fluctuations is determined by the strength of the interactions between 2D droplets. The interaction energy between two circular stress domains decays as the inverse cube of their separation [33],

$$U(r_{ij}) = g\frac{A_i A_j}{r_{ij}^3}, \tag{1}$$

where A_i is the area of 2D droplet i, and r_{ij} is the distance between 2D droplets i and j. Assuming an isotropic elastic substrate, the interaction strength g is defined by

$$g = \frac{(\Delta\sigma)^2(1-\nu^2)}{\pi E}, \tag{2}$$

where $\Delta\sigma$ is the difference in surface stress between the overlayer and surface alloy phases, and E and ν are the Young's modulus and Poisson's ratio of the substrate, respectively. The 2D-droplet fluctuations can be used to determine g (and thus $\Delta\sigma$) in the following manner. First, we pick one 2D droplet. By measuring the instantaneous positions and areas of all of the surrounding 2D droplets, we use Eq. (1) to predict the equilibrium position of the 2D droplet under consideration. We then calculate the deviation of the measured instantaneous position from the predicted position. Figure 2(b) shows a probability distribution of one spatial component of these deviations for three 2D-droplet configurations. In compiling these distributions, typically arrays of 200 2D droplets at 600 different times were analyzed. Notice that the width of the distribution depends strongly on the 2D-droplet density, and relatively weakly on the temperature over the temperature range where the self-assembly is observed. We will show that the strong density dependence is accounted for by Eq. (1), while the weak

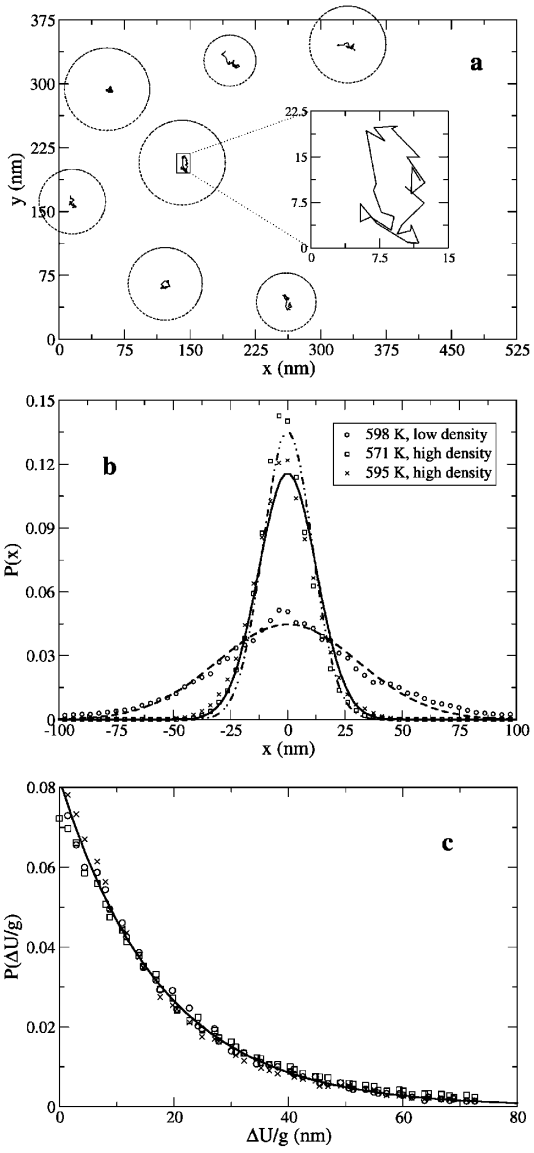

FIG. 2. (a) Example trajectories that were measured for several different 2D droplets from 15 consecutive images of a fairly ordered 2D-droplet configuration at 595 K. Dashed circles are drawn to provide an indication of the area of the 2D droplets. (b) Distribution of the displacements of the 2D droplets under different conditions. The 2D-droplet density for the high density data is a factor 2.7 times higher than that of the low density data. (c) The probability distribution of $\frac{\Delta U}{g}$, determined from the analysis as it is described in the text. Despite the difference in experimental conditions, all three data sets collapse onto one single curve (solid line).

temperature dependence is due to a temperature-independent $\Delta\sigma$ in Eq. (2).

To estimate g from the data, instead of plotting distributions of the spatial deviation, we plot distributions of the thermal excitation energy ΔU, defined as the calculated energy of the 2D droplet minus the equilibrium energy. Figure 2(c) shows the distribution of $\Delta U/g$ corresponding to the 2D-droplet configurations of Fig. 2(b). There are two remarkable features of these distributions. First, they are consistent with the exponential Boltzmann statistics one expects from thermal fluctuations; i.e., the probability of ΔU is proportional to $e^{-(\Delta U)/(kT)}$. Second, the distributions are almost identical for different temperatures and densities. From Eqs. (1) and (2), this implies a constant $\Delta\sigma$. Table I lists the values of $\Delta\sigma$ obtained by fitting the distribution to $e^{-(\Delta U)/(kT)}$, and using Eq. (2) to obtain $\Delta\sigma$, with values of 130 GPa and 0.34 for E and ν. The average, 1.21 N/m (76 meV/Å^2), is of a reasonable order of magnitude when compared to stress differences measured for most of the low-index single crystal metal surfaces [34,35]. Notice also that the interaction between 2D droplets is the same as between inverted 2D droplets. This equality is consistent with the interactions being caused by the stress mismatch at the boundary.

The constancy of $\Delta\sigma$ is significant in light of previous work showing that the feature size is strongly temperature dependent [30]. For elastically stabilized domains, the feature size is

$$l_0 = \pi a e^{\{(\pi E\beta)/[(\Delta\sigma)^2(1-\nu^2)]\}+1}, \quad (3)$$

where β is the boundary energy per unit length and a is the domain boundary width [18]. The temperature dependence could thus be due to a variation in either $\Delta\sigma$ or β. The lattice constant of the Pb in the overlayer phase varies significantly with temperature [27,29]. Given this variation, one might have expected similar variations in $\Delta\sigma$. Apparently, the structural changes in the Pb overlayer phase do not lead to a significant variation of the stress difference. A temperature-independent stress difference between the two phases implies that the changing periodicity has to be attributed to a changing boundary energy. This observation is supported by measurements of the thermal fluctuations of the boundaries [36].

TABLE I. Estimated stress differences.

Type	T (K)	$\Delta\sigma$ (N/m)
Inverted 2D droplet	623	1.45 ± 0.21
Inverted 2D droplet	615	1.12 ± 0.18
Inverted 2D droplet	628	1.18 ± 0.18
Inverted 2D droplet	632	1.24 ± 0.18
Inverted 2D droplet	598	1.06 ± 0.15
2D droplet	571	1.09 ± 0.15
2D droplet	595	1.30 ± 0.18

In our analysis of the thermal motion of 2D droplets, we explicitly assume that the interaction between the 2D droplets is dipolar in nature. We now support this assumption by comparing our observations of the 2D droplet-stripe phase transition with predictions of dipolar-interaction models [1,2,4,7,9,10,17–24]. According to Ng and Vanderbilt [23], if the boundaries between the two surface phases are sharp, the transitions between the 2D droplet to stripe to inverted 2D-droplet phases occur at area fraction 0.29 and 0.71. Here the "area fraction" is defined as the fraction of the total surface area that is covered by the overlayer phase. Figure 3(a) shows measured total areas for the 2D droplets, stripes, and inverted 2D droplets vs area fraction for deposition at 673 K. The criterion used to classify a domain as a 2D droplet or a stripe is that a stripe has an area at least twice

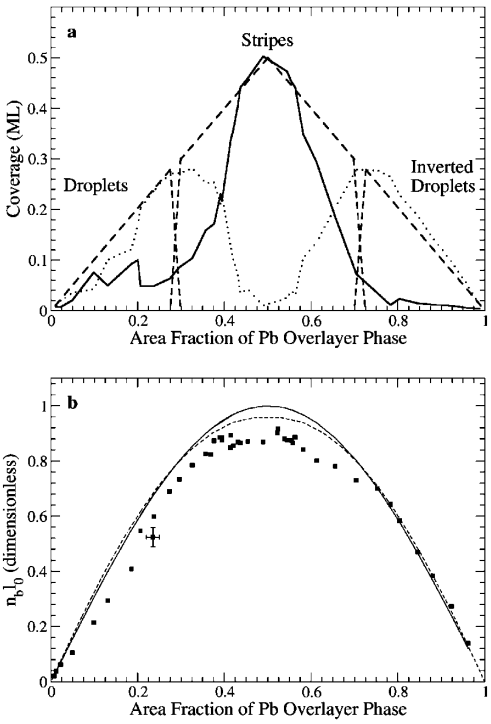

FIG. 3. Comparison of the area-fraction dependence of the domain patterns with a dipolar interaction model. (a) Measured total coverages of the 2D droplets (dotted, left), the inverted 2D droplets (dotted, right), and the stripes (solid) as a function of area fraction at 673 K showing the phase transitions between the 2D-droplet and stripe phases. Data points have reproducibility based errors in both x and y of about 7%. Curves predicted by theory are plotted as dashed lines. (b) Domain boundary density as a function of the area fraction of the overlayer phase. The data points are the measured densities, n_b, times the characteristic stripe width, l_0, plotted versus the area fraction, f, at 673 K. One data point has the data set error bars marked. Pb depositions at 630, 651, and 691 K yielded similar data. The solid and dashed lines are theoretical predictions [23] for the stripes and (inverted) 2D droplets, respectively, assuming sharp interfaces between domains.

the mean 2D-droplet area measured over the deposition run. In fact, the observed widths of the 2D droplet-stripe transitions are larger than those predicted by theory. Nonetheless, the onsets of the transition regions are in reasonable accord with the predicted first order phase transitions. Thermal excitations, observed in both the 2D droplet and stripe phases (but not included in the zero-temperature theory), are most likely responsible for the differences in the transition width.

Another prediction of the dipolar model, which can be tested with our data, concerns the domain boundary density, n_b (domain length per unit area), as a function of area fraction, f. The prediction is that n_b first increases then decreases as the system evolves from 2D droplets to stripes to inverted 2D droplets [12,19,21–24]. The feature size l_0 defines the length scale in the theory and equals the stripe width in the equilibrium stripe phase at $f = 0.5$. Our LEEM images provide a direct means to determine the domain boundary density and the value of l_0. Figure 3(b) shows the theoretical curve [23] and experimental results for deposition at 673 K. Similar plots indicate only small variations with temperature from 630 to 691 K. Again, the agreement is reasonable, considering the neglect of entropic effects in the theory [23]. Combined with our measurement of the phase transitions and our analysis of the 2D-droplet motion, this is convincing evidence of the elastic nature of the interactions in the Pb/Cu(111) system.

In summary, we have analyzed the thermal fluctuations of self-assembled Pb structures on Cu(111). This analysis has enabled us to show that the long-range repulsive interactions responsible for self-assembly are quantitatively consistent with an elastic model. This conclusion of the importance of substrate relaxations complements similar conclusions about the forces responsible for size selection in domain patterns on Si(111) [37]. The stress difference is found to be temperature independent, suggesting the observed temperature dependent feature size is due to a varying boundary energy. Thus, the energetics governing the temperature-coverage phase diagram can be understood quantitatively. An open question is the microscopic origin of the stress difference we find. This question could be addressed by a first-principles calculation of the stresses. Such calculations are in progress [38].

The authors thank Peter Feibelman, Brian Swartzentruber, and François Léonard of Sandia National Laboratories for useful discussions. This work was supported by the Department of Energy, Office of Basic Energy Sciences, Division of Materials Science and Engineering, and was performed at Sandia National Laboratories, a multiprogram laboratory operated by Sandia Corporation, a Lockheed Martin company, for the United States Department of Energy under Contract No. DE-AC04-94AL85000.

[1] M. Seul and D. Andelman, Science **267**, 476 (1995).
[2] T. Garel and S. Doniach, Phys. Rev. B **26**, 325 (1982).
[3] M. Seul and R. Wolfe, Phys. Rev. A **46**, 7519 (1992).
[4] S. A. Langer, R. E. Goldstein, and D. P. Jackson, Phys. Rev. A **46**, 4894 (1992).
[5] A. B. Kashuba and V. L. Pokrovsky, Phys. Rev. B **48**, 10 335 (1993).
[6] A. J. Dickstein *et al.*, Science **261**, 1012 (1993).
[7] D. J. Keller, H. M. McConnell, and V. T. Moy, J. Phys. Chem. **90**, 2311 (1986).
[8] D. Andelman, F. Brochard, and J. -F. Joanny, J. Chem. Phys. **86**, 3673 (1987).
[9] H. M. McConnell, Annu. Rev. Phys. Chem. **42**, 171 (1991).
[10] S. L. Keller and H. M. McConnell, Phys. Rev. Lett. **82**, 1602 (1999).
[11] K. Kern *et al.*, Phys. Rev. Lett. **67**, 855 (1988).
[12] P. Zeppenfeld *et al.*, Surf. Sci. **342**, L1131 (1995).
[13] K. Pohl *et al.*, Nature (London) **397**, 238 (1999).
[14] H. Ellmer *et al.*, Surf. Sci. **476**, 95 (2001).
[15] G. E. Thayer *et al.*, Phys. Rev. Lett. **86**, 660 (2001).
[16] R. Plass *et al.*, Nature (London) **412**, 875 (2001).
[17] V. I. Marchenko, JETP Lett. **33**, 381 (1981).
[18] O. L. Alerhand, D. Vanderbilt, R. D. Meade, and J. D. Joannopoulos, Phys. Rev. Lett. **61**, 1973 (1988).
[19] M. M. Hurley and S. J. Singer, Phys. Rev. B **46**, 5783 (1992).
[20] D. Vanderbilt, Surf. Sci. Lett. **268**, L300 (1992).
[21] C. Sagui and R. C. Desai, Phys. Rev. E **49**, 2225 (1994).
[22] A. D. Stoycheva and S. J. Singer, Phys. Rev. E **65**, 036706 (2002).
[23] K.-O. Ng and D. Vanderbilt, Phys. Rev. B **52**, 2177 (1995).
[24] C. Sagui and R. C. Desai, Phys. Rev. E **52**, 2807 (1995).
[25] J. Henrion and G. E. Rhead, Surf. Sci. **29**, 20 (1972).
[26] G. Meyer, M. Michailov, and M. Henzler, Surf. Sci. **202**, 125 (1988).
[27] B. H. Müller, Th. Schmidt, and M. Henzler, Surf. Sci. **376**, 123 (1997).
[28] C. Nagl *et al.*, Surf. Sci. **321**, 237 (1994).
[29] Y. S. Chu, I. K. Robinson, and A. A. Gewirth, Phys. Rev. B **55**, 7945 (1997).
[30] R. Plass, N. C. Bartelt, and G. L. Kellogg, J. Phys. Condens. Matter **14**, 4227 (2002).
[31] E. Bauer, Rep. Prog. Phys. **57**, 895 (1994).
[32] R. A. Plass and G. L. Kellogg, Surf. Sci. **470**, 106 (2000).
[33] J. M. Rickman and D. J. Srolovitz, Surf. Sci. **284**, 211 (1993).
[34] H. Ibach, Surf. Sci. Rep. **29**, 193 (1997).
[35] Corrections to Eq. (2) due to the elastic anisotropy of the Cu substrate are on the order of 10% [F. Léonard and N. C. Bartelt (to be published)].
[36] R. van Gastel, N. C. Bartelt, and G. L. Kellogg (to be published).
[37] R. M. Tromp and J. B. Hannon, Surf. Rev. Lett. **9**, 1565 (2002).
[38] P. J. Feibelman (private communication).